

$^{194}\text{Pt}(d, ^3\text{He})^{193}\text{Ir}$ reaction: Spectroscopic factors and supersymmetry predictions

Y. Iwasaki, E. H. L. Aarts, M. N. Harakeh, R. H. Siemssen, and S. Y. van der Werf

Kernfysisch Versneller Instituut, University of Groningen, Groningen, The Netherlands

(Received 10 November 1980)

Differential cross sections have been measured for transitions to low-lying states in ^{193}Ir in the $^{194}\text{Pt}(d, ^3\text{He})^{193}\text{Ir}$ reaction at $E_d = 50$ MeV. Transferred orbital angular momenta l and spectroscopic factors have been deduced by comparison with zero-range distorted-wave Born-approximation calculations. The deduced spectroscopic factors give further evidence for the presence of the supersymmetric structure in nuclei in the platinum region, which has been recently pointed out by Iachello. The spin-parity of a state at $E_x = 0.964$ MeV has been assigned to be $1/2^+$.

[NUCLEAR REACTIONS $^{194}\text{Pt}(d, ^3\text{He})^{193}\text{Ir}$, $E = 50$ MeV, measured $\sigma(\theta)$, resolution] 30 keV. DWBA analysis, deduced l and S .

I. INTRODUCTION

Low-lying states in odd- A nuclei in the platinum region are interesting in the light of various models,^{1,2} in particular the recently proposed supersymmetry model.³ It has been pointed out as evidence of the presence of the supersymmetric structure in the Pt region that the observed states can indeed be grouped into bands as predicted by the supersymmetry model, and that a closed supersymmetry energy-level formula reproduces the experimental energy levels of both $^{192}\text{Pt}_{114}$ and $^{191}\text{Ir}_{114}$ at the same time.³ Additional evidence for the presence of the supersymmetry is given by the agreement between predicted $E2$ transition rates⁴ and measured ones.⁵ A further possible test of the presence of the supersymmetry in the Pt region is provided by a comparison of predicted transfer-reaction intensities⁴ with experimental values.

Proton-hole components of low-lying states in ^{193}Ir were previously studied by the $^{194}\text{Pt}(t, \alpha)^{193}\text{Ir}$ reaction at $E_t = 15$ MeV.² The (t, α) reaction at incident energies of about 15 MeV, however, can give no information on the transferred orbital angular momenta l , because the angular distribution shapes are uncharacteristic of l , these being rather similar for $l=0-5$.² Therefore, it is impossible to conclude from the angular distribution shape that the mechanism of a (t, α) transition is a direct single-step pickup with a single l value. Spectroscopic factors were obtained,² assuming J^π values that had been proposed earlier. Because of these difficulties with the (t, α) reaction and the current interest in the supersymmetry model, we felt it important to study the proton pickup on ^{194}Pt independently via a different reaction that is free from these shortcomings. Therefore we undertook an experimental study of the $^{194}\text{Pt}(d, ^3\text{He})^{193}\text{Ir}$ reaction.

II. EXPERIMENTAL PROCEDURE AND RESULTS

A self-supporting ^{194}Pt target with a thickness of about $300 \mu\text{g}/\text{cm}^2$ was bombarded by an energy-analyzed beam of 50 MeV deuterons from the Kernfysisch Versneller Instituut (KVI) isochronous cyclotron. The QMG/2 magnetic spectrograph⁶ and the associated particle-detection system⁷ were used to detect and identify the ^3He particles. An overall energy resolution of ~ 30 keV was obtained with a solid angle of 8.5 msr, which was defined by an entrance aperture of the spectrograph with a horizontal opening angle of $\sim 6^\circ$.

Figure 1 shows a ^3He momentum spectrum taken at $\theta_{\text{lab}} = 15^\circ$. The positions of peaks 1–12 as numbered in Fig. 1 are consistent with the excitation energies given in a recent compilation⁸ as well as

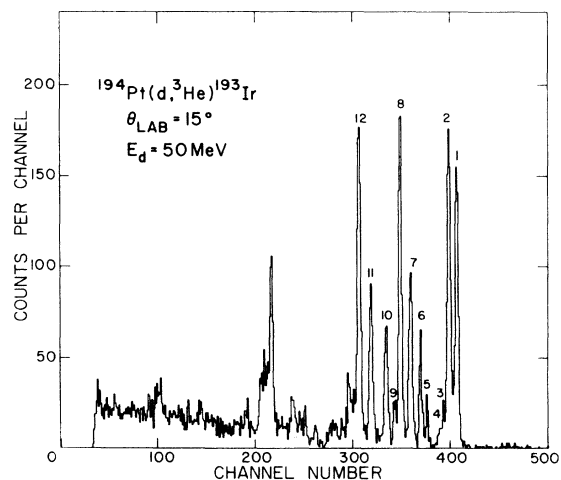


FIG. 1. Momentum spectrum of ^3He particles from the reaction $^{194}\text{Pt}(d, ^3\text{He})^{193}\text{Ir}$. Peak No. 1 corresponds to the ground state, and peak No. 12 to a state at $E_x = 0.964$ MeV in ^{193}Ir .

with those obtained by the previous $^{194}\text{Pt}(t, \alpha)^{193}\text{Ir}$ experiment.² Because of the high level density at excitation energies above 1 MeV, there it was impossible to resolve peaks reliably and to obtain angular distributions with characteristic l values. In particular, the peak around channel 218 in Fig. 1 is remarkably large, but the angular distribution obtained for it was flat, indicative of contributions of a number of l values. Therefore, the data analysis was limited to the twelve peaks below 1 MeV. A summary of the observed states is given in Table I.

Figure 2 shows the experimental differential cross sections obtained for the twelve peaks numbered as in Fig. 1. The absolute cross section scale has been determined by normalizing to the differential cross sections for deuteron elastic scattering. It is seen that each of the twelve angular distributions has a shape characteristic of a transferred orbital angular momentum l , in contrast with the (t, α) angular distributions.

III. DISTORTED-WAVE BORN APPROXIMATION ANALYSIS

A distorted-wave Born approximation (DWBA) analysis of the present data has been performed

TABLE I. Summary of observed states.

Peak No.	E_x^a (MeV)	$J\pi^a$	l^b
1	0.000	$\frac{3}{2}^+$	2
2	0.073 0.080	$\frac{1}{2}^+$	0
		$\frac{11}{2}^-$	
3	0.139	$\frac{5}{2}^+$	2
4	0.180	$\frac{3}{2}^+$	2
5	0.299	$\frac{7}{2}^-$	3
6	0.358 0.362	$\frac{7}{2}^+$	2
		$(\frac{5}{2}^+)$	
7	0.460	$\frac{3}{2}^+$	2
8	0.557 0.559	$\frac{1}{2}^+$	2
		$(\frac{5}{2}^+)$	
9	0.621	$\frac{7}{2}^+$	4
10	0.695 0.712	$(\frac{5}{2}^+)$	2
		$(\frac{3}{2}^+)$	
11	0.849 0.874		2
12	0.964	$(\frac{1}{2}, \frac{3}{2})$	0

^aReference 8.

^bPresent work. See text.

with the zero-range DWBA code DWUCK 4.⁹ The employed potential parameters are given in Table

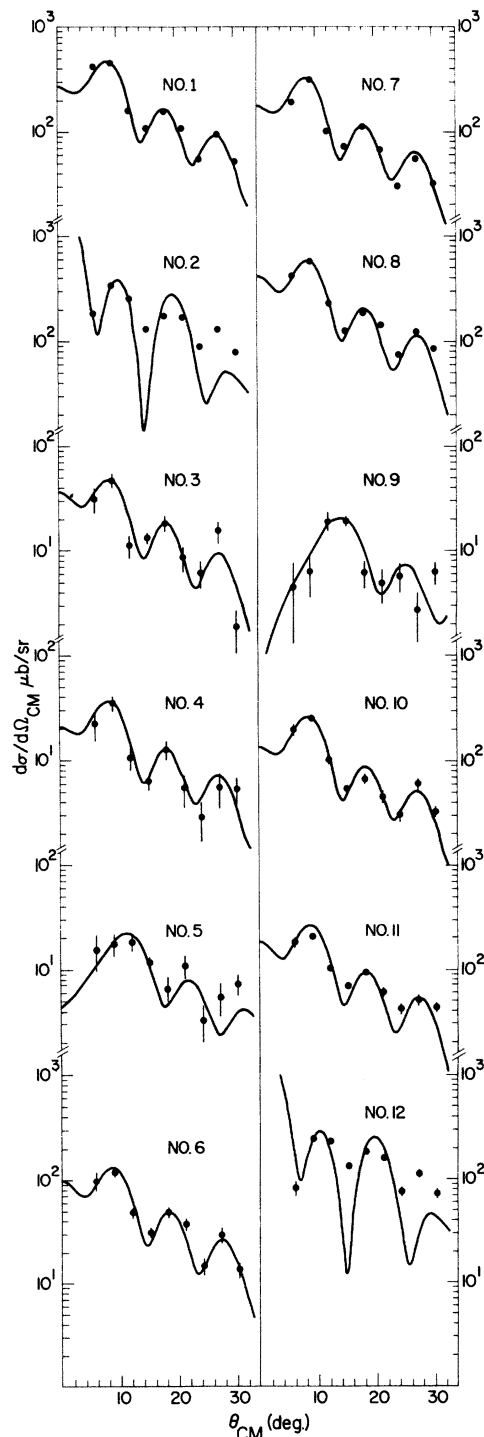


FIG. 2. Differential cross sections for transitions to low-lying states in ^{193}Ir in the $^{194}\text{Pt}(d, ^3\text{He})^{193}\text{Ir}$ reaction at $E_x = 50$ MeV. (See Table I for the numbering of states in ^{193}Ir and for the assigned l values.) The solid curves represent results of DWBA calculations (see text).

TABLE II. Set of potential parameters used in the DWBA calculation.

	V (MeV)	W_D (MeV)	W (MeV)	V_{SO} (MeV)	r_0 (fm)	r'_0 (fm)	r_{SO} (fm)	a (fm)	a' (fm)	a_{SO} (fm)
d	91.0	14.25	0.0	6.0	1.16	1.25	1.16	0.83	0.90	0.83
^3He	168.0	0.0	17.0	0.0	1.24	1.52		0.723	0.88	
p	varied ^a	0.0	0.0	$\lambda=25$	1.225		1.225	0.70		0.70

^aThe proton single-particle wave function is calculated by the well-depth method.

II. The calculated angular distributions are shown by solid lines in Fig. 2. No finite-range and non-locality corrections were applied. The deuteron optical parameters were taken from the literature.¹⁰ The combination of these deuteron parameters with the ^3He optical parameters of Ref. 10, which had given good fits for the $^{208}\text{Pb}(d, ^3\text{He})^{207}\text{Tl}$ reaction,¹¹ failed to reproduce the experimental angular distributions of Fig. 2, especially the peak-height ratio of the first peak to the second one of the $l=2$ angular distributions (for example, No. 1 of Fig. 2). Therefore, an extensive study was performed of the dependences of the calculated angular distributions on the parameters of the potentials including the proton-binding potential. The ^3He optical parameters of Table II came out of this study, which confirmed at the same time the stability of the calculated angular distributions and consequently the reliability of the l assignment based on the angular distribution shape. On the other hand, the absolute value of the calculated cross section is quite unstable as dependent on the potential parameters. For example, it was found that a small change in the radius parameter of the proton-binding potential (a few percent; for example, from 1.225 to 1.250 fm) could change the absolute value of the calculated cross section by a large amount (several tens of percent) without a substantial change in the angular distribution shape. This instability of the calculated absolute cross section implies a large inherent uncertainty in the absolute spectroscopic factor deduced by a DWBA analysis, since it is by no means possible to determine the radius parameter of the proton-binding potential with a high accuracy (a few percent or better).

A summary of l assignments by the present DWBA analysis is included in Table I. Although each of the peaks 2, 6, and 8 corresponds to two unresolved states, the angular distribution shape indicates that one of the two states is populated far more strongly than the other. The l values determined by the present DWBA analysis are consistent with the previous spin-parity assignments⁹ (Table I). Furthermore, the spin-parity of the 0.964 MeV state (Table I) is uniquely determined to be $\frac{1}{2}^+$ by the $l=0$ assignment to the transi-

tion to this state. This spin-parity assignment contradicts the suggestion of Yamazaki *et al.*² that there exists a strongly populated $\frac{3}{2}^+$ state at $E_x = 0.970$ MeV as the bandhead of the Nilsson configuration [402]. The above $l=0$ assignment is based on the following observations: (1) the features of the experimental angular distribution (No. 12 of Fig. 2), including the sharp fall of the differential cross section at 6° , are consistent only with an $l=0$ DWBA curve, and (2) the experimental angular distribution is very similar to that for the known $l=0$ transition to the 0.073 MeV state (No. 2 of Fig. 2).

Spectroscopic factors have been derived using the relation

$$C^2S = \frac{\sigma_{\text{exp}}}{2.95\sigma_{\text{DWUCK}}/(2j+1)},$$

where j is the total angular momentum of the proton single-particle orbital, and $C^2=1$. The absolute spectroscopic factors, which are reported in the third column of Table III, are subject to large uncertainties arising from ambiguities in the potential parameters. However, the uncertainties in the *relative* spectroscopic factors for states corresponding to the *same* proton single-particle orbital are within $\pm 5\%$. Relative spectroscopic factors, normalized so that the spectroscopic factor for the ground state transition is unity, are shown in Table III for the reactions $^{194}\text{Pt}(d, ^3\text{He})^{193}\text{Ir}$ (column 4) and $^{194}\text{Pt}(t, \alpha)^{193}\text{Ir}$ (column 6). There is good agreement between the relative spectroscopic factors derived from both reactions. Thus, the present experimental study of the $(d, ^3\text{He})$ reaction confirms the earlier results from the (t, α) reaction, and therefore gives evidence that the mechanism of the (t, α) reaction around $E_t = 15$ MeV is a direct single-step pickup.

IV. COMPARISON WITH SUPERSYMMETRY PREDICTIONS

The presence of the supersymmetry leads to simple expressions that predict relative spectroscopic factors for single-nucleon-transfer transitions connecting an even target nucleus with some final states in the residual nucleus. In the classification scheme of the supersymmetry model the

TABLE III. Spectroscopic factors for low-lying states in ^{193}Ir .

Orbital	E_x (MeV)	$(d, ^3\text{He})$		(t, α)			
		S^a abs.	S'^c rel.	$S(t, \alpha)^b$ abs.	$S'(t, \alpha)^c$ rel.		
$2d_{3/2}$	0.000	1.17	1.00	0.64	1.00		
	0.180	0.09	0.08	0.03	0.05		
	0.460	0.87	0.74	0.46	0.72		
	0.712 ^d	0.30 ^e	0.26	0.15	0.23		
		0.73 ^f	0.62				
$2d_{5/2}$	0.849 ^h	0.74	0.63	0.05	0.08		
	0.874 ^h						
	0.139	0.09	0.08			0.05	0.08
	0.362	0.25	0.21			0.15	0.23
	0.559	1.15	0.98			0.69	1.08
	0.695 ^d	0.31 ^e	0.26				
		0.52 ^g	0.44				
	0.849 ^h	0.56	0.48			0.37	0.58
0.874 ^h	0.03			0.05			
$3s_{1/2}$	0.073	0.43 ⁱ	0.37	0.24	0.38		
	0.964	0.41	0.35				
$2f_{7/2}$	0.299	0.03	0.02				
$1g_{7/2}$	0.621	0.24	0.21	0.15	0.23		

^aPresent work. See text.

^bReference 2.

^cDerived from the preceding column by normalizing so that the spectroscopic factor for the ground state transition is unity.

^dThe 0.695 and 0.712 MeV states were not resolved in the present $(d, ^3\text{He})$ experiment, being observed as peak No. 10.

^eThis spectroscopic factor is obtained if the cross section for peak No. 10 (Table I, Fig. 2) is divided into the cross sections for the 0.695 and 0.712 MeV states according to the ratio observed in the (t, α) reaction (Ref. 2).

^fThis is obtained if the whole cross section for peak No. 10 is assumed to belong to the 0.712 MeV state.

^gThis is obtained if the whole cross section for peak No. 10 is assumed to belong to the 0.695 MeV state.

^hSpins of these states are not established. The present work assigns $l=2$ to the summed angular distribution for the states (Table I).

ⁱPossible $l=5$ excitation of the 0.080 MeV ($\frac{1}{2}^-$) state is neglected in the derivation of the spectroscopic factor for the 0.073 MeV state, since it is unfeasible to deduce a small $l=5$ admixture from an analysis of the shape of angular distribution No. 2 (see text, Table I, and Fig. 2). This neglect could lead to an uncertainty of less than 10% in the spectroscopic factor for the 0.073 MeV state. For example, if a substantial spectroscopic factor of $S'=2.39$ were assumed for the 0.080 MeV ($\frac{1}{2}^-$) state according to an estimate of Ref. 2, the 0.080 MeV ($\frac{1}{2}^-$) state would contribute 8% of summed differential cross sections at 9° to 10° c.m. where the first peak of summed angular distribution No. 2 (Fig. 2) is located.

three lowest $\frac{3}{2}^+$ states in ^{193}Ir at $E_x=0.000$, 0.180, and 0.460 MeV have the Spin(6) and Spin(5) quantum numbers $[\sigma_1, \tau_1]$ of $[\frac{1}{2}, \frac{1}{2}]$, $[\frac{1}{2}, \frac{5}{2}]$, and $[\frac{1}{2}, \frac{1}{2}]$,

respectively.^{3,4} The corresponding quantum numbers of the ground state of ^{194}Pt are $[7, 0]$. The transition to the 0.180 MeV state in the $^{194}\text{Pt}(d, ^3\text{He})^{193}\text{Ir}$ reaction should be forbidden by the selection rules $\Delta\sigma_1 = \pm \frac{1}{2}$ and $\Delta\tau_1 = \pm \frac{1}{2}$ for single-nucleon-transfer reactions,⁴ and this transition is indeed observed to be weak. More precisely, the supersymmetry model predicts⁴ the ratios between the spectroscopic factors for the ground ($\frac{3}{2}^+$), 0.180 MeV ($\frac{3}{2}^+$), and 0.460 MeV ($\frac{3}{2}^+$) states in ^{193}Ir (Tables I and III) to be $1:0:N/(N+4) \equiv 1.00:0.00:0.64$, where $N=7$ is the number of bosons in the target nucleus ^{194}Pt . The predicted ratios are in qualitative agreement with the corresponding experimental ratios $1.00:0.08:0.74$ (Table III). On the other hand, according to the calculations of Ref. 2, the rotation-vibration model and the Nilsson model predict the ratios to be, respectively, $1.00:0.09:1.09$ and $1.00:0.22:0.31$. While complicated models such as the above ones containing a large number of adjustable parameters may be able to reproduce the experimental relative spectroscopic factors, it is interesting that the supersymmetry predictions which depend on no adjustable parameters at all are in at least as good a qualitative agreement with the experimental relative spectroscopic factors. The present results thus provide further evidence for the presence of the supersymmetry in nuclei of the Pt region.

The supersymmetry model of Iachello deals with the coupling of a $j = \frac{3}{2}$ particle (or hole) with an even-even core that has the $O(6)$ symmetry. It does not include single-particle excitations other than $j = \frac{3}{2}$. Other states arising from a $2d_{5/2}$ particle (or hole) or a $3s_{1/2}$ particle (or hole) coupled with the $O(6)$ core, which are beyond the scope of the supersymmetry model, may be admixed into the observed low-lying states that can be classified according to the supersymmetry scheme. Our experimental data indicate the presence of such admixtures. For example, the 0.362 MeV ($\frac{3}{2}^+$) and 0.073 MeV ($\frac{1}{2}^+$) states are excited with considerable strengths in single-proton pickup, whereas the excitation of these states is forbidden in the supersymmetry model by the selection rule $\Delta\tau_1 = \pm \frac{1}{2}$ because $[\sigma_1, \tau_1] = [\frac{1}{2}, \frac{5}{2}]$ and $[\frac{1}{2}, \frac{3}{2}]$, respectively, for the 0.362 MeV ($\frac{3}{2}^+$) and 0.073 MeV ($\frac{1}{2}^+$) states.^{3,4} The experimental results indicate the presence of considerable $2d_{5/2}$ and $3s_{1/2}$ hole strengths in these states. It remains to be seen whether a fully quantitative reproduction of the experimental spectroscopic factors can be achieved by a calculation that takes account of admixtures of the $2d_{5/2}$ and $3s_{1/2}$ single-particle excitations in the framework of the interacting boson-fermion model.¹

The authors acknowledge stimulating discussions with F. Iachello and O. Scholten. The present work has been performed as part of the research program of the Stichting voor Fundamen-

teel Onderzoek der Materie (FOM) with financial support of the Stichting voor Zuiver Wetenschappelijk Onderzoek (ZWO).

¹F. Iachello and O. Scholten, Phys. Rev. Lett. 43, 679 (1979); Kernfysisch Versneller Instituut Report No. KVI-220, 1979.

²Y. Yamazaki, R. K. Sheline, and D. G. Burke, Z. Phys. A 285, 191 (1978), and references therein.

³F. Iachello, Phys. Rev. Lett. 44, 772 (1980).

⁴F. Iachello, private communication.

⁵M. N. Harakeh, P. Goldhoorn, Y. Iwasaki, J. Łukasiak, L. W. Put, S. Y. van der Werf, and F. Zwarts, Phys. Lett. 97B, 21 (1980), and references therein.

⁶A. G. Drentje, H. A. Enge, and S. B. Kowalski, Nucl. Instrum. Methods 122, 485 (1974); A. G. Drentje, R. J. de Meijer, H. A. Enge, and S. B. Kowalski, *ibid.*

133, 209 (1976).

⁷J. van der Plicht and J. C. Vermeulen, Nucl. Instrum. Methods 156, 103 (1978).

⁸*Table of Isotopes*, 7th ed., edited by C. M. Lederer and V. S. Shirley (Wiley, New York, 1978), pp. 1237 and 1238.

⁹P. D. Kunz (unpublished).

¹⁰W. C. Parkinson, D. L. Hendrie, H. H. Duhm, J. Mahoney, J. Saudinos, and G. R. Satchler, Phys. Rev. 178, 1976 (1969).

¹¹Reference 10 used a lower cutoff radius of 8.8 fm. No lower radial cutoff is used in the present work.